Cytometry 24:14–26 (1996)

Quantitative Analysis of Three-Dimensional Distribution of AgNOR Proteins During Interphase in Leukemic Cells

Z.M. Wozniak, Y. Usson, F. Parazza, P. Champelovier, D. Leroux, and D. Seigneurin

Equipe de Cytologie Quantitative (Z.M.W., P.C., D.S.), Service de Cytogénétique (D.L.), DyOGen & TIMC-IMAG (Y.U., F.P.), Université Joseph Fourier, Grenoble, France; and Department of Pathology, University of Wroclaw, Poland (Z.M.W.)

Received for publication September 27, 1994; accepted January 8, 1996

Acidic proteins of the nucleolar organizer regions, selectively stained by silver (AgNOR-proteins), were investigated during interphase in leukemia cells with a confocal scanning laser microscope (CSLM). Simultaneous confocal fluorescence (for specific labeling of DNA, using propidium iodide) and transmitted light microscopy combined with digital deconvolution (for the location of the AgNOR proteins in nonconfocal mode) were used. The distribution of the AgNOR proteins measured by 3D microscopy was described by their number, the volume occupation of the nucleus by the AgNOR aggregates, the distance between each AgNOR, the distance of each AgNOR to the nucleolar border, and their anisotropy. The results of the 3D analysis were compared to those obtained by conventional 2D analysis, cytogenetical analysis of metaphase nucleolar organiser regions (NORs), and cell duplication rate. The descriptive power of these 3D parameters were assessed for nine leukemic cell lines. The measurements of the 3D spatial distribution of AgNORs was a better discriminant parameter than the morphological parameters (i.e., number and volume). The 3D expression of AgNORs is also a reliable parameter for assessing proliferative activity of leukemic cells and seems to be in relation with the differentiation stage of these leukemic cells. © 1996 Wiley-Liss, Inc.

Key terms: NORs, Ag-NOR proteins, three-dimensional study, 3D reconstruction, quantification, nucleolus

Nucleolar organizer regions (NORs) are the genomic DNA segments encoding for ribosomal RNA (rRNA) (40). In human somatic cells, NORs are located on the short arms of the five acrocentric chromosomes; numbers 13, 14, 15, 21, and 22 (20, 24). During interphase, the NORs are located in the fibrillar center and surrounding dense fibrillar components of nucleoli (9). They can be visualized in chromosome preparation and in interphase nuclei because each NOR is associated with argyrophilic proteins (AgNOR) involved in the regulation of transcription or post-transcriptional modification of rRNA transcripts (21, 47). The silver staining technique for the demonstration of NORs (AgNORs) was originally used to demonstrate NORs in cytogenetic preparations (18, 23). The technique was simplified and first applied to histological and cytological preparations by Ploton et al. (38). Recently, it has been demonstrated that the quantity of interphase AgNORs is related to the cell proliferation rate, allowing the use of interphase AgNOR quantification as a parameter for cell kinetics evaluation (11, 12, 55). Sequential in situ hybridization of rRNA genes and AgNOR staining studies showed that AgNOR proteins can be considered to be a marker of ribosomal genes that are actively transcribed or potentially active (24, 41, 47). However, it has been demonstrated that the distribution of interphase AgNORs can be useful to distinguish malignant cells from corresponding benign or normal cells on the basis of a higher quantity of interphase AgNORs (7, 31, 51). The AgNORs are considered to represent a new, additional diagnostic and prognostic information in tumour pathology (13, 15).

The aim of this work was to compare the usually employed 2D quantification of AgNORs with 3D quantification and distribution of the nucleolar argyrophilic components during interphase in leukemic cells lines. The 3D spatial distribution of AgNORs was investigated using simultaneous confocal laser scanning fluorescence (nuclear staining by propidium iodide) and transmitted light

This work was partly supported by the Ligue Départamentale contre le cancer de Haute-savoie and the ligue départamentale de l'Isère.

Address reprint requests to Z.M. Wozniak, Equipe de Cytologie Quantitative, Laboratoire de Génétique, Histologie et Biologie de la Reproduction, Faculté de Médecine de Grenoble, 38700 La Tronche, France.

microscopy combined with digital deconvolution (for the location of AgNOR proteins in non confocal mode). The results of the 3D analysis were compared to those obtained by conventional 2D analysis, cytogenetical analysis of metaphase nucleolar organizer regions, cell duplication rate, and differentiation stage of nine leukemic cell lines. To our knowledge, it is the first quantitative approach of the 3D spatial distribution of AgNOR proteins in interphase leukemic cells.

MATERIALS AND METHODS

Cell Culture

Nine leukemia continuous cell lines—LAMA 84 (46), LAMA 87 (6), LAMA 88 (6), HL60 (16), U937 (48), THP-1 (52), K562 (29), UM384 (5), NB4 (28)—derived from leukemic patients were investigated. Cell lines were maintained in suspension culture (RPMI 1640 medium, Boehringer Mannheim, Meylan, France) supplemented with 10% of Fetal Bovine Serum (FBS—Gibco; Cergy Pontoise, France), 100 IU/ml penicillin, and 100 mg/ml streptomycin in a humidified atmosphere (5% CO2, 95% air) at 37°C. The medium was changed twice weekly.

Population Doubling Time

Cells (5×10^5) were grown in plastic flasks. The population doubling times were determined by counting the cells in triplicate samples at 24-hr intervals according to the method described by Patterson (37).

Staining for Karyotyping

G, R, and C banding was performed to ascertain the karyotype. Twenty metaphase cells from each sample were analysed according to ISCN (27). Total chromosome number and acrocentric chromosome number were counted and the mean calculated. In the K562 cell line, the number of acrocentric chromosomes could not be determined (great heterogeneity).

NORs Staining of Cytogenetic Samples

Silver staining of NORs was carried out on cytogenetic samples using a solution of 1 vol 2% gelatine in 1% aqueus formic acid and 2 vol 50% silver nitrate. Silver staining was performed for 20 min at room temperature (18–20°C) in the dark. After staining, the slides were rinsed in a 5% thiosulfate solution, washed in bi-distilled deionized water, and stained with 4% Giemsa for 10 min. The NORs in metaphase cells were counted and the mean number calculated (20 cells per cell line). In U937, NORs number cannot be evaluated.

Preparation and Analysis of Samples in 2D for Conventional Light Microscopy

Cytocentrifuged cell samples were air dried, fixed in 100% ethanol, and stained with selective one-step silver staining technique for the AgNOR proteins following the procedure reported by Ploton (39, 40). After rehydration, the slides were covered with a freshly made staining solution prepared by mixing two solutions: one volume of a 2% gelatin solution in 1% formic acid and two volumes of 50% $AgNO_3$. The slides were incubated for 25 min at room temperature in the dark. After staining, they were washed in bi-distilled water and placed in 5% sodium thiosulphate solution for 5 min. After fixation in thiosulphate solution, they were rinsed in bi-distilled water, counterstained with Mayer's haematoxylin for 5 s, dehydrated in graded alcohols, and cleared in xylol. All solutions were prepared in glassware cleaned with an acid dichromate solution. Quantitative 2D analysis was performed with a computer-assisted image analysis system (SAMBA 2005, Alcatel-TITN Co., Grenoble, France). The images obtained by a CCD video camera mounted on light microscope (Axioplan, Zeiss, Germany) were displayed on a TV screen. Measurements were made with a plant-apochromat ×100/1.0 oil immersion objective (Zeiss); the total magnification was ×1250. Video signals were digitized and stored as 512 × 512 pixels coded in 256 levels of gray.

Analysis in Confocal Microscopy

Preparation of samples for observation in confocal microscopy. For 3D analysis and in order to preserve the nuclear volume, the cells were fixed in paraformaldehyde, stained with selective one-step silver staining technique for the AgNORs proteins, and counterstained with propodium iodide (PI). In brief, 2 ml of suspension culture containing 1×10^6 cells were centrifuged for 5 min at 800 rpm and resuspended in 4% paraformaldehyde for 10 min. The slides were treated with aminoalkysilane (42) to enhance adherance. Approximately 5×10^4 cells were applied per slide and centrifuged at 700 rpm for 5 min using a Cytospin (Shandon). The preparation was washed for 10 min in deionized water and stained with selective one-step silver staining technique for the AgNOR proteins, as noted previously (39), and rinsed again in water. Propidium iodide solution (50 μg/ml) was used for DNA specific labelling for 20 min. The slides were then washed three times in distilled water and mounted with antifading solution (2.3% w/v DABCO in 90% glycerol 0.1 M Tris. pH 7.5). Finally a 20 × 20 mm coverslip was sealed with nail polish.

Data acquisition. The optical sections of the AgNOR proteins and the nucleus were acquired simultaneously using a LSM410 confocal scanning laser inverted microscope (Carl Zeiss, Oberkochen, Germany) fitted with a 63 ×, NA 1.4, Plan-Apochromat oil immersion objective. The AgNOR proteins were imaged in laser scanning brightfield transmitted light mode, whereas the nucleus (propidium iodide stained) was imaged in confocal laser scanning fluorescence mode. Propidium iodide fluorescence (nuclear imaging) was excited with the 514 nm wavelength of an Argon laser. The emitted red fluorescence was collected through a 560 nm beam splitter followed by a 590 nm long-pass filter. The same laser wavelength was used for the transmission mode (AgNOR proteins imaging) to avoid differences in focal planes. The voxels were sampled every 0.12 μm in the focal plane; the microscope stage was moved vertically up 0.24 μm between the recording of each optical section; and

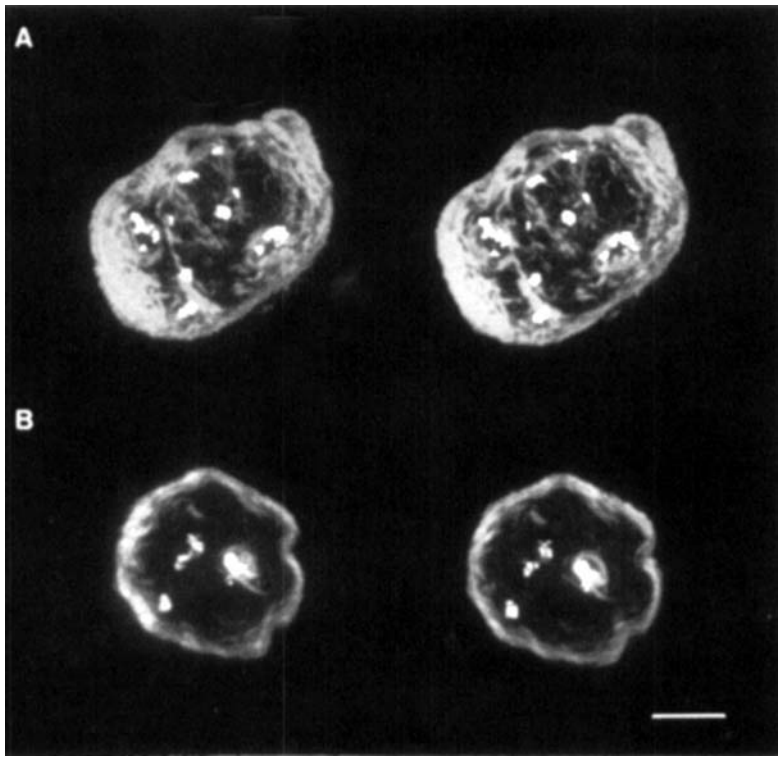

FIG. 1. Examples of 3D reconstructions of nuclei and AgNORs. **A.** Stereogram of a Lama 87 cell nucleus; the nuclear envelope is shown in gray and the AgNOR can be seen in bright white (15 aggregates). **B.** Stereogram of a HL-60 cell nucleus; only 6 aggregates can be seen. Scale bar: 5 μm.

the quantification of signal intensity was done on 8 bits (256 gray level values). Each optical section was recorded with a scanning time of 0.5 s per field. This scanning time was long enough to obtain a good signal to noise ratio while limiting the fading of the PI fluorescence. For each sample, the optical sections were stored as two series of 60 digital images (128 × 128 pixels): one corresponded to the sections of the nucleus (NV volume) and the other corresponded to the sections of AgNOR proteins (AG volume).

Computer equipment. The discrete values were transferred and stored on a workstation via a high-speed IEEE-488 communication line. Since the amount of data was huge, they were archived on a digital audio tape device (1.2 Gbyte per tape). The analysis of the discrete volumes were performed on an Iris Indigo workstation (Silicon Graphics, Mountain View, CA). This UNIX workstation was fitted with a RS 4000 RISC processor and a 64 Mbytes RAM.

The analysis software and 3D visualisation software (Fig. 1) were written in standard C language using the GL library (Silicon Graphics library) and the FORMS user interface library (courtesy of Marck Overmars, Department of Computer Science, Utrecht University, The Netherlands). We developed a program to extract measurements from the 3D data sets. The features were: (1) morphological parameters such as the number of Ag-NOR stained aggregates, their average volume fraction and the associated standard deviation, (2) topographical parameters such as the normalised average distance of the Ag-NOR stained aggregates from the nuclear border, the normalised average distance to the nearest neighbour of each aggregate, and their respective standard deviations; and (3) anisotropical parameters given by the two first latent roots eigenvalues of the matrix of direction cosines (35) (Fig. 2, Table 1).

Because the AgNOR stack of sections was collected in a nonconfocal mode, the axial resolution was much lower than that obtained for the nuclear stack. To compensate for the difference of resolution, a restoration process was performed on the first data set. This restoration filter (36) is based on a simplified implementation of the nearest-neighbour method (4) (Fig. 3). We assessed the efficiency of the restoration process by comparing the result of the segmentation of AgNORs on a few nuclei after deconvolution, with the result of the segmentation of the same data directly imaged in confocal reflection contrast. An example of such comparison is shown in Figure 4. It appears that the result of the segmentation is quite similar in both cases, although a finer resolution is obtained in confocal reflection contrast. After this restoration step, the Ag-NOR stained aggregates were segmented by a gray level thresholding. Then the connected components corresponding to each AgNOR stained aggregate were labeled using a seed-fill algorithm (36). After this labelling step, the volume of each aggregate was

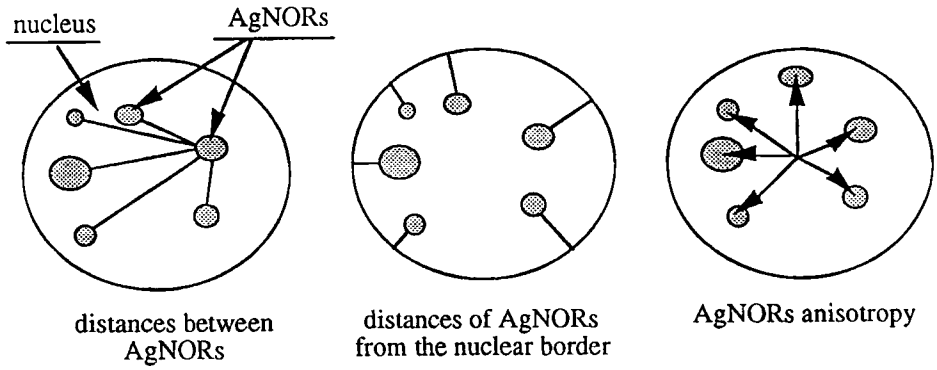

FIG. 2. Schematic diagram of the topographical features extracted from the 3D data sets.

Table 1
Thirteen Parameters Computed on AgNORs 3D Images

Parameters	Abbreviation
Morphological parameters	
Number of aggregates	NbNOR
Average volume fraction (%)	AV
Scatter of volume fraction	SV
Average total volume fraction	ATV
Scatter of total volume fraction	STV
Topographical parameters	
Normalised average distance of the Ag-NOR aggregates from the nuclear border	ADE
Scatter of normalised distance of the Ag-NOR aggregates from the nuclear border	SDE
Normalised average of interaggregates distances	AD
Scatter of normalised interaggregates distances	SD
Normalised average distance to the nearest neighbour of each aggregate[a]	AN
Scatter of normalised distance to the nearest neighbour of each aggregate[a]	SN
Anisotropical parameters	
1st eigenvalue	EV1
2nd eigenvalue	EV2

[a]Parameters rejected by discriminant analysis.

calculated by counting the number of voxels with the same label. To compute distances between aggregates, distances from the border of the nucleus and other topographical parameters to the center of gravity of each labeled aggregate were calculated.

A bias due to the high opacity of the silver staining was clearly seen on the nuclear sections: the AgNOR staining aggregates created a shadowing effect beneath their locations in the nuclear sections. The fluorochromes located under the aggregates were not uniformly excited and the light they emitted was partially blocked. This effect resulted in conical shadows under the locations of the AgNOR stained aggregates in the nuclear sections. Consequently, before the calculations of features, the presumed boundaries of the nucleus had to be retrieved. We chose to approximate the boundaries of the nucleus by its convex hull. The convex hull calculation was based on the Voronoi diagram (3, 35). The shadowing effect did not create a real problem for the calculation of the center of gravity of the AgNOR aggregates since in transmitted light microscopy the level of light is many orders of magnitude greater than in fluorescence and the amount of diffracted light collected by the lens under the aggregates is sufficient to form a complete image of the volume.

In order to avoid measurement biases induced by the different sizes of nuclei, all the distances were normalised by a reference distance. This unitary distance *Dnorm* was the shortest distance between the nuclear gravity centre and the border of the nucleus. The shortest distance of each aggregate was normalised with this reference distance. For each nucleus, the average and standard deviation were computed for the distance between each pair of aggregates and the distance of each aggregate to its closest neighbour.

The morphological parameters were the number of AgNOR aggregates, the average volume fraction of AgNOR aggregates, and the associated standard deviation. The volume fraction was calculated by dividing the volume of an aggregate by the volume of the convex hull of the nucleus.

To measure the anisotropy of the distribution of AgNOR stained aggregates in the nucleus, we defined 3D unitary vectors along the directions originating from the gravity centre of the nucleus and pointing to each gravity centre of AgNOR stained aggregates (Fig. 2). The measurement of the anisotropy of the spatial distribution of aggregates was given by the values of the two first latent roots (or eigenvalues) of the matrix of direction cosines of these vectors. This method was introduced by Anderson and Stephens (1). The relative proportions of the eigenvalues EV1 and EV2 indicate the degree of anisotropy. For example, for a perfect isotropy EV1 and EV2 are equal to 33%; when the anisotropy increases EV1 becomes significantly greater than EV2 (35).

RESULTS

AgNOR Analysis and Cell Duplication Rate

The correlation between the mean of three measurements of the doubling time and the mean of the number of interphase AgNORs is shown in Figure 5. The mean

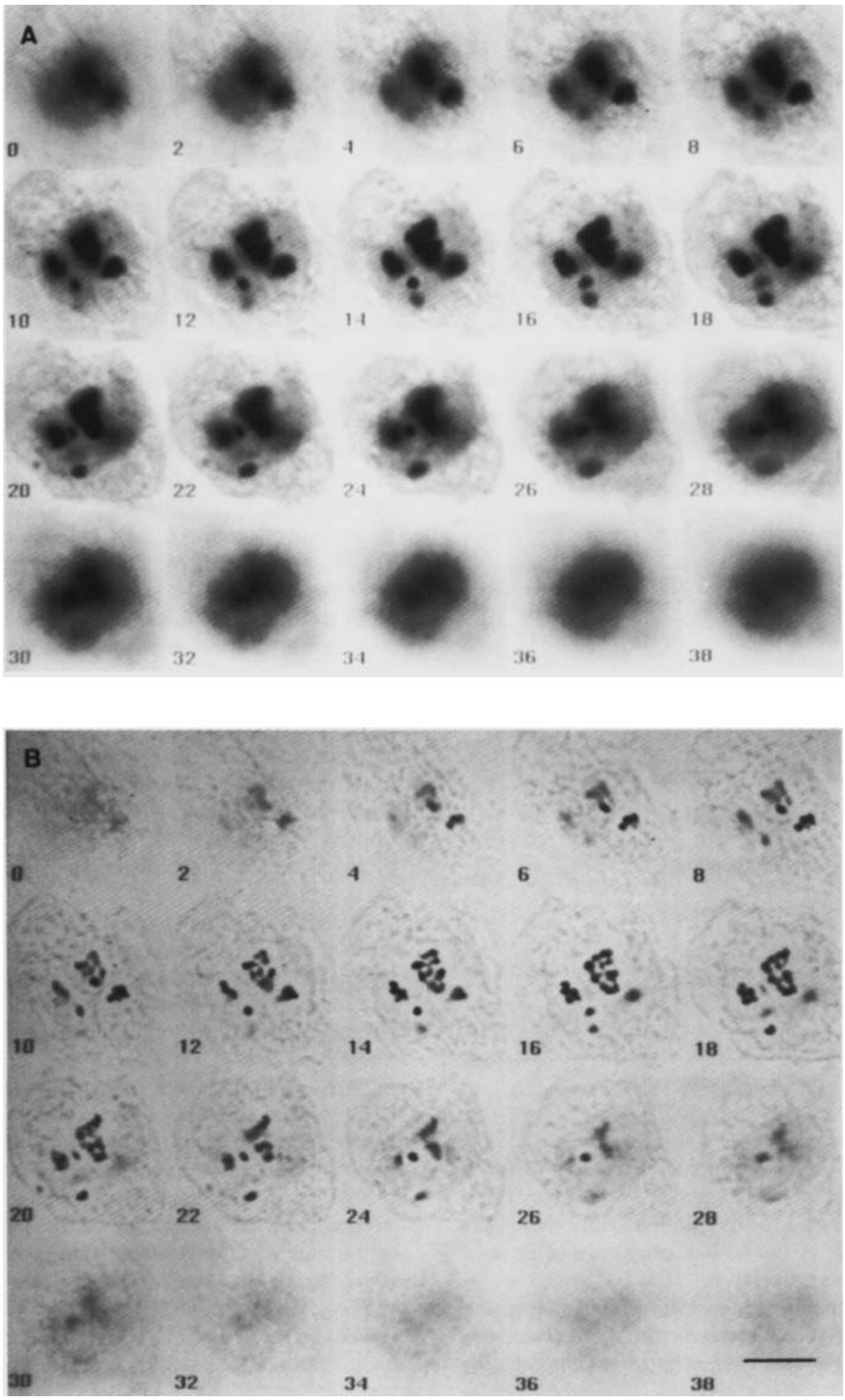

FIG. 3. Example of serial optical sections of AgNORs in a nucleus of a Lama 87 cell in transmitted light microscopy. **A.** Raw images of every second section (0.48 μm apart) along the optical axis. **B.** Deblurred images of the same sections obtained by digital deconvolution. Scale bar: 5 μm.

doubling time showed a greater correlation with the mean number of AgNORs in 3D ($r = 0.94, P < 0.0001$) than in 2D analysis ($r = 0.86, P < 0.003$). The nine cell lines were separated into three groups: (1) with a doubling time under 23 h, (2) between 26 and 29 h, (3) 31 h or more. In the first group (fast proliferating cell lines

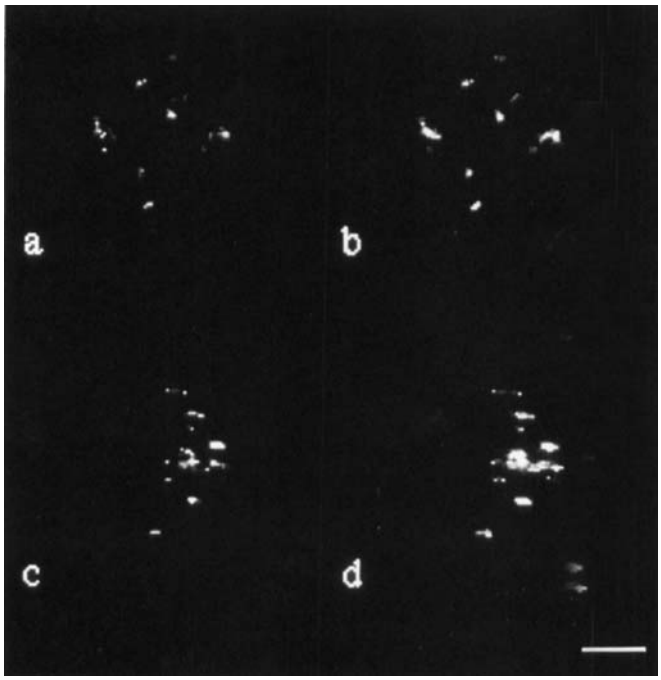

FIG. 4. Comparison of the segmentation of the AgNOR aggregates of the same nucleus imaged with different microscopical modes: left column (**a,c**), confocal reflection contrast; right column (**b,d**), deconvolved transmitted light microscopy. Top row (**a,b**): 3D reconstruction view facing the optical axis (z axis). Bottom row (**c,d**): 3D reconstruction view after a 90° rotation about the y axis. Scale bar: 5 μm.

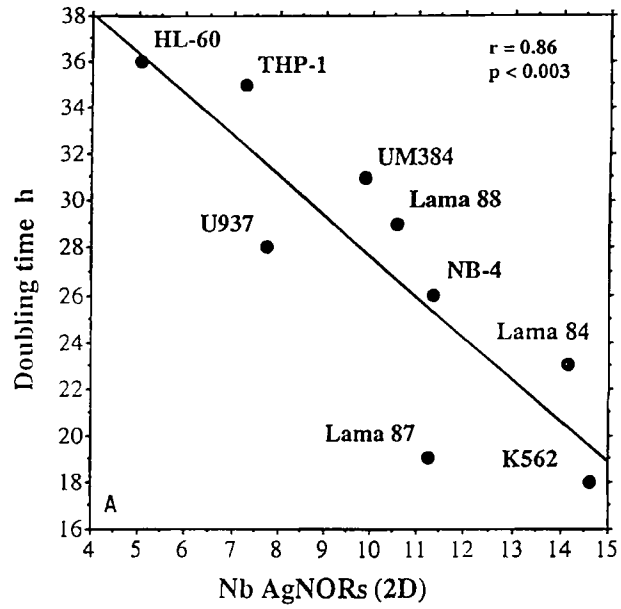

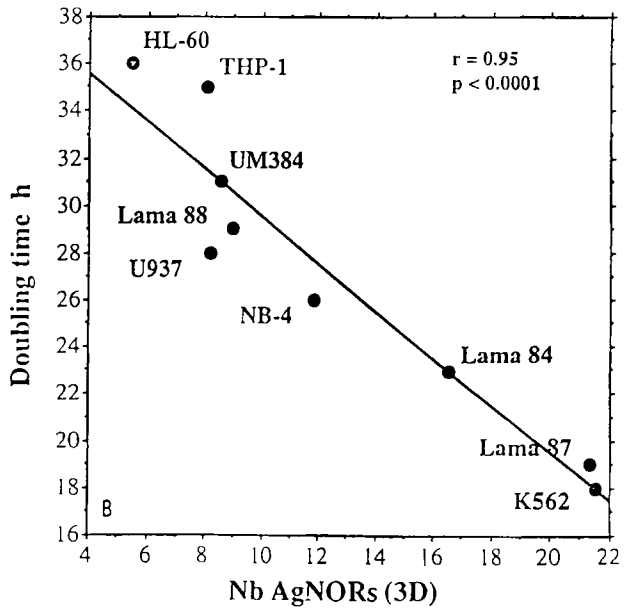

FIG. 5. Correlation between the AgNOR number (NbAgNORs) and the cell duplication rate in 2D analysis [$y = -1.75x + 45.06$; $r^2 = 0.74$] (**A**) or 3D analysis [$y = -0.98x + 39.01$; $r^2 = 0.89$] (**B**).

(K562, Lama 87, Lama 84), one can observe a considerable difference between the number of AgNORs measured in 2D and in 3D (13.33 ± 5.38, 19.79 ± 5.38, respectively). In the second and third groups, corresponding to slow proliferating cells, no significant differences were observed (2) 2D 9.88 ± 2.94, 3D: 9.67 ± 3.02); (3) 2D: 7.53 ± 2.75, 3D: 7.39 ± 2.08). Comparisons of the doubling time with the AgNOR areas in 2D (Fig. 6A) showed a greater correlation than the AgNOR number measured in the same mode ($r = 0.92$, $P < 0.0005$). This correlation was not observed with the average total volume fraction (ATV) (Fig. 6B).

3D AgNOR Analysis vs. Cytogenetical Analysis

A significant correlation was found between interphase AgNORs determined by 3D analysis and NOR number on metaphase cells ($r = 0.69$, $P < 0.05$). Interphase AgNORs also showed a positive but not statistically significant trend with the number of metaphase acrocentric chromosomes ($r = 0.67$, $P < 0.06$). However, AgNOR number in 3D was not correlated with the total number of chromosomes ($r = 0.55$, $P < 0.1$) (Fig. 7).

2D vs. 3D AgNORs Analysis

The number of AgNORs detected by 3D analysis was generally greater than in 2D (Fig. 8). The major significant differences were observed in Lama 87 (3D: 21.28 ± 7.59; 2D: 11.23 ± 3.06) and K562 (3D: 21.51 ± 6.02; 2D: 14.62 ± 3.77). These two cell lines had the fastest cell duplication rate (Fig. 5). Only in Lama 88 (3D: 9 ± 2.6, 2D: 10.56 ± 3.39) and UM384 (3D: 8.53 ± 3.25, 2D: 9.86 ± 2.4), the AgNORs number measured by 3D quantification was lower than in 2D analysis. The mean of the volume of AgNORs computed in 3D was not correlated with the area of AgNORs in 2D analysis ($r = 0.45$, $P < 0.2$) (Fig. 9).

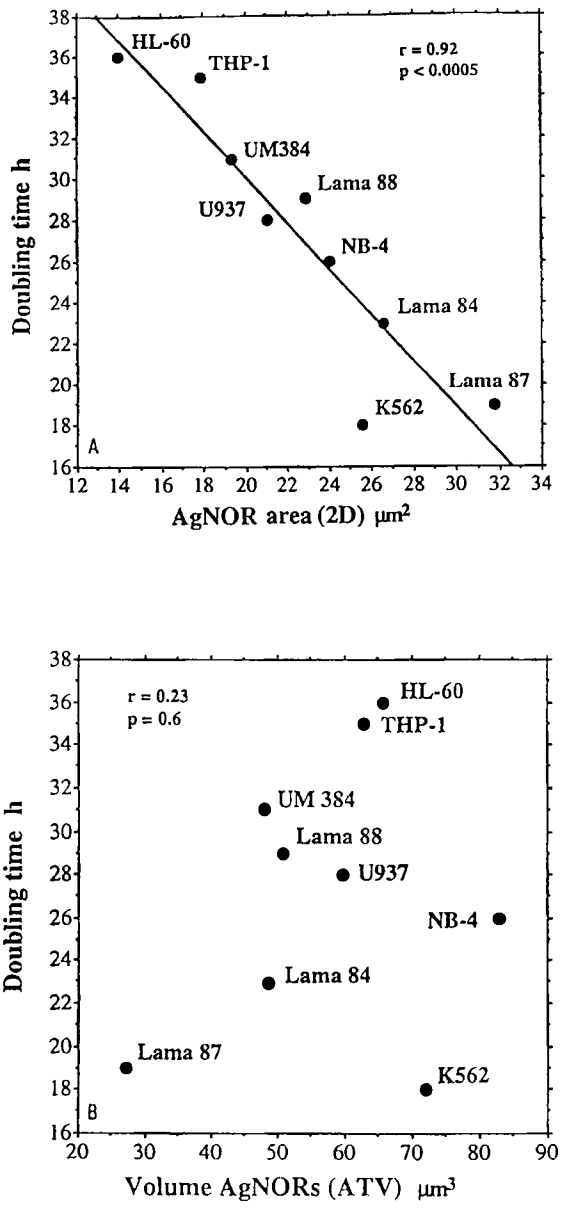

FIG. 6. Correlation between the cell duplication rate and the mean of AgNOR area measured in 2D [$y = 0.01 \times + 52.45$; $r^2 = 0.84$] (A) and mean of total volume of AgNOR (ATV) (B).

Analysis of Spatial Distribution Parameters

Statistical analysis. The AgNOR proteins were selectively detected by specific silver staining and nuclear DNA by propidium iodide. The silver stained proteins were visualized in enhanced transmitted light microscopy (nonconfocal mode) and the PI fluorescence of the

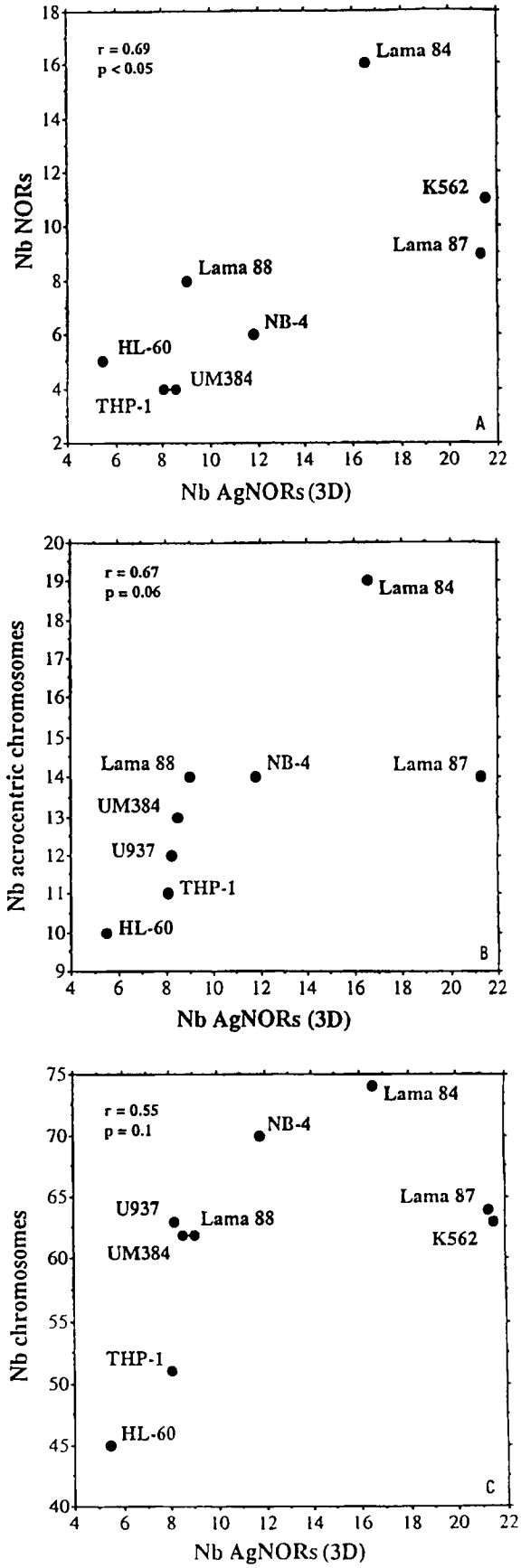

FIG. 7. Correlation between the mean of AgNOR number computed in 3D and the number of NORs in metaphase cells (A), the acrocentric chromosome number (B), or the total chromosome number (ploidy) (C).

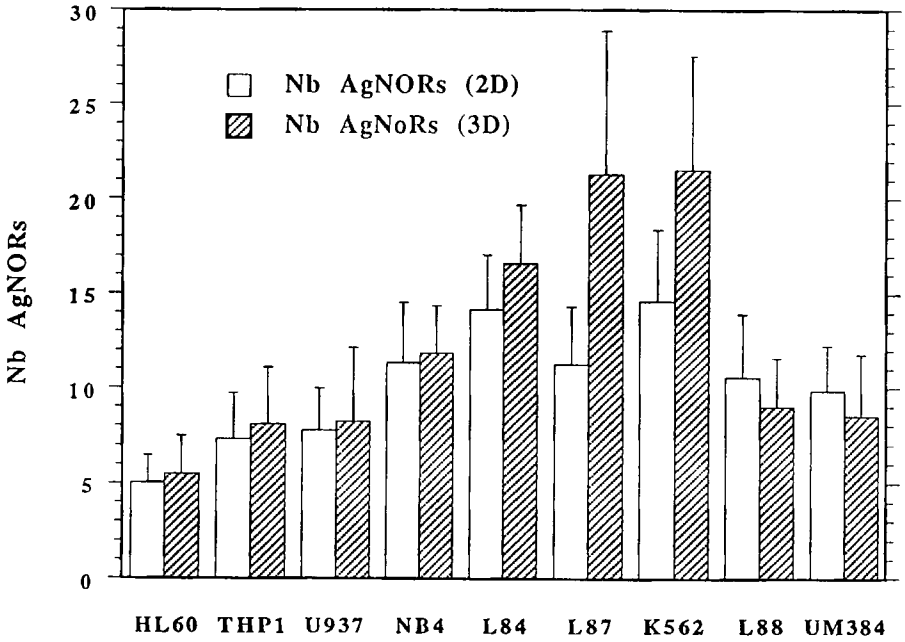

FIG. 8. Comparisons of the mean of AgNOR number in each cell lines obtained by 2D and 3D analysis. Bars correspond to the standard deviations.

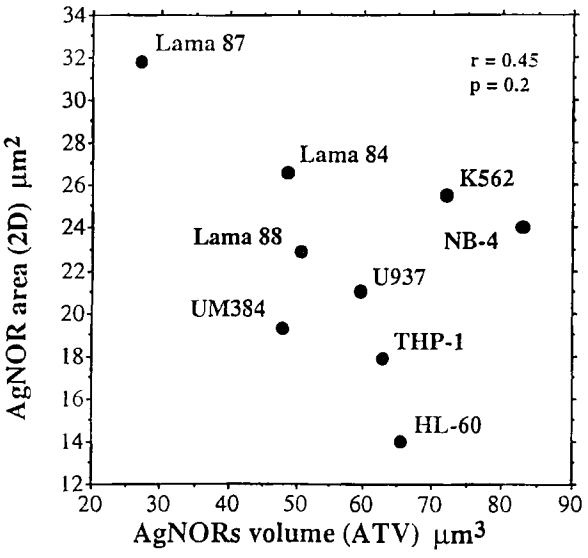

FIG. 9. Comparisons of the mean of AgNOR area measured in 2D with the average total volume fraction (ATV) of AgNOR in 3D.

nucleus in confocal mode. To study the spatial distribution of AgNOR proteins, we defined a series of parameters that quantify the topography, the morphology, and the anisotropy (Table 1). The analysis of all spatial distribution parameters showed the following trends: In all analysed cell lines, the first anisotropical parameter (1st eigenvalue—EV1) was much greater than the second anisotropical parameter (2end eigenvalue—EV2); the means for each cell line was approximately the same (EV1 ≅ 55%, EV2 ≅ 30%) (Fig. 10A). The normalised average distance from nuclear border (ADE) and scatter of normalised distance from nuclear border (SDE) demonstrated that excepting the K562 cell line, the majority of AgNORs are located midway between the center of the nuclear mass and the nuclear border (AgNORs of K562 were more frequently located on the periphery) (Fig. 10B). This suggested that AgNOR aggregates were situated preferentially in the central and equatorial plane. The longest distances between AgNOR aggregates (normalised average distance—AD, scatter of normalised distance—SD) were found in HL-60, whereas the shortest were found in Lama 87. Generally, the inter-AgNOR distances were longer in slow proliferating cell lines (Fig. 10C). A similar tendency was observed in the distribution of the volume fractions (average volume fraction—AV, scatter of average volume fraction—SV); the average volume fraction of AgNOR aggregates was smaller in the fast proliferating cells than in slow proliferating cells (Fig. 10D).

Factorial discriminant analysis. To recapitulate the differences or resemblances between the nine cell lines, we used a factorial discriminant analysis (FDA). The parametric description of each cell lines was used as the basis for defining a Bayesian cell classifier. After such a classifier was obtained, each cell was submitted to it and reassigned to the cell line it had the highest probability of belonging to. The percentage of good reclassification is a way to assess the measurement accuracy. The higher this percentage, the more discriminant the parameters are. The most discriminatory parameters were the AgNOR number (NbNOR; discriminant power/dp = 68.853) and normalised average distance from nuclear border (ADE; dp = 21.033); the less discriminatory was the second

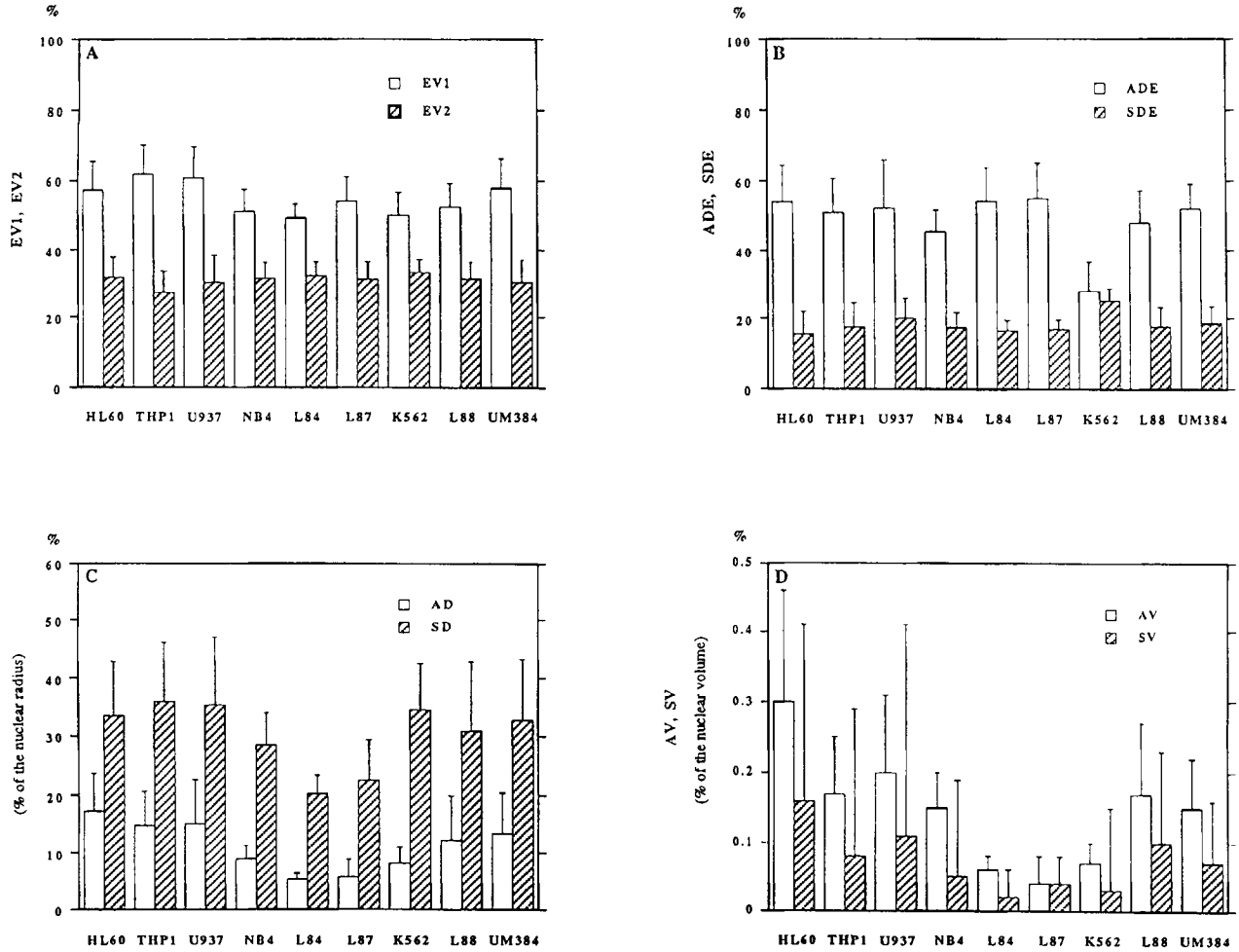

FIG. 10. Comparisons of the parameters computed on 3D images. **A.** Anisotropical parameters: first eigenvalue EV1 and second eigenvalue EV2. Bars correspond to the standard deviations. The ordinate axis is expressed as a percentage of the sum of the three eigenvalues. **B.** Topographical parameters: normalised average distance of the AgNOR aggregates from the nuclear border ADE and scatter of normalised distance of the AgNOR aggregates from the nuclear border SDE. **C.** Normalised average of inter-aggregates distances AD, scatter of normalised inter-aggregates distances SD. **D.** Morphological parameters: average volume fraction AV and scatter of volume fraction SV. Bars correspond to the standard deviations.

anisotropical parameter (EV2; dp = 1.663). Table 2 shows the rate of well-classified cells (bold figures) for each group after the ninth step of a stepwise discriminant analysis using the Bayesian classifier. The rate of good reassignment (or total correct classification rate) was 74.5%. This high value confirmed the significance of the measurements. Indeed, if these were not representative and cells were reclassified randomly, the rate of good reassignment would be 11%. The two remaining variables (normalised average distance—AN and scatter of normalised distance—SN to the nearest neighbour of each aggregate) did not significantly improve the classification. In our study the most individualized cells lines were K562, Lama 84, and NB4. The most frequently misclassified cell lines were Lama 88 and U937. Figure 11 represents the projections of 9 cell lines (95% tolerance ellipses) on the first and the second factorial planes defined by FDA. On the first factorial plane three groups of cell lines can be distinguished: i—HL60, Lama 88, NB4, THP1, U937, UM384, ii— K562, iii = Lama 87, Lama 84. The first group corresponds to the slowly proliferating cell lines, the second and third correspond to highly proliferating cells. On the second factorial plane, the differences between the cell lines belonging to the first group were more visible.

DISCUSSION

Recently AgNOR proteins have become a new parameter to assess cellular proliferation. The nature and relationship between interphase AgNOR quantity and cellular proliferation have been widely investigated under different conditions and models of cellular and tumoral pathology (13, 15, 49). In the cell lines derived from different tumour types, it has been demonstrated that

Table 2
Confusion Matrix for 9 Cell Lines[a]

	HL60	THP-1	UM384	Lama 88	U937	NB-4	Lama 84	Lama 87	K562
HL60	**21**	4	3	3	1	0	0	0	0
THP-1	3	**24**	4	2	0	1	0	1	0
UM384	0	2	**23**	2	1	3	0	1	0
Lama88	3	2	3	**18**	0	7	3	1	0
U937	3	5	3	0	**15**	0	0	3	0
NB-4	0	0	0	0	0	**29**	2	0	0
Lama84	0	0	0	0	0	0	**29**	1	0
Lama87	0	0	2	0	0	1	2	**24**	0
K562	0	1	1	0	0	0	0	0	**33**

[a]Confusion matrix. Total correct classification rate: 74.5%. Classification of AgNORs labeled nuclei was obtained after the ninth stage of a stepwise discriminant analysis using 11 topographical variables. The two remaining variables (AN and SAN) did not significantly improve the correct classification rate. In such a matrix, the rows correspond to the actual cell line and the columns correspond to the groups to which the nuclei were assigned to by a Bayesian classifier. Bold face numbers on the main diagonal indicate the number of well-classified nuclei. For example, in the K562 cell line, 33 cells were correctly identified, whereas one cell was confused with THP-1 and one cell was confused with UM384.

rapidly proliferating cells have an amount of interphase AgNOR proportionally higher than slowly proliferating cells and that AgNOR quantity can be considered as an indicator of the speed of the cell duplication (11, 44, 49). To assess the relationship between AgNOR expression and cellular proliferation, the AgNOR quantity was compared to the kinetic data obtained by evaluation of other cell proliferation markers. A significant correlation or positive trend was shown between the AgNOR quantity and tumour growth fraction expressed by percentage of the S-phase cells in non-Hodgkin's lymphoma (8), breast carcinoma (17), gastric carcinoma (44), and meningiomas (34). However, this correlation was not observed in leukemia cells labeled with bromodeoxyuridine (33). A significant correlation was observed between AgNOR values and growth fraction evaluated by the nuclear Ki-67 immunoreactivity in numerous human tumours (13, 15, 49). Similar studies investigated the relationship between metaphase NORs and the quantity of the interphase AgNOR proteins (10, 12). These data indicated the lack of direct relationship between metaphase NOR numbers, the number of NORs bearing chromosomes, and interphase AgNOR quantity in neoplastic cells. Most of the nucleolar organizer regions analyses in the leukemic cells refer to metaphase NORs (2, 12) or to interphase AgNORs (19, 32, 33), whereas few studies refer to both (30). In bone marrow, the number of metaphase NORs was higher in lymphoblastic leukemia than in normal cells (2). Metaphase NOR and interphase AgNOR scores were studied in chronic myeloid leukemia (30). AgNOR numbers demonstrated greater variations in bone marrow than in peripheral blood cells, which more closely resemble normal lymphocytes. However, the NOR numbers diminished in the most mature cells. Large variations of NOR and AgNOR scores were observed in acute nonlymphoblastic leukaemias (45). In all the above mentioned reports, the quantitative approach was evaluated under 2D conditions. Therefore, it is reasonable to suppose that the "absolute" number of AgNOR (more frequently calculated) was underestimated. On the contrary, the AgNOR area is artefactually overestimated. Both errors of estimation are related to resolution limitations. To verify this hypothesis, we proposed a quantitative approach of 3D spatial distribution of AgNORs in leukemic cell lines using simultaneous confocal laser scanning fluorescence (nuclear staining by PI) and improved transmitted light microscopy (AgNOR proteins in nonconfocal mode). The results of the 3D analysis were also compared to cell duplication rates and to the number of NOR sites and of acrocentric chromosomes, and to the total chromosome number (cytogenetic study). Three recent studies presented 3D data (22, 37, 43). Although these were only qualitative, they provided interesting information about the organization of AgNORs, the transcriptional regions, and the nucleolus. Other authors such as Imamura et al. (26) used a fluorescent NOR (FINOR) staining and measured the NOR expression in 3D (number, diameter) on histological sections of benign, borderline, and malignant human tumours. They observed a remarkable increase of FINORs in the process of tumour progression.

AgNOR Analysis and Cell Duplication Rate

In our study the number of AgNORs estimated under 3D spatial conditions showed a greater correlation with cell duplication rate than that calculated in 2D. The differences in AgNOR enumeration were particularly obvious in rapidly proliferating cell lines. The average total volume fraction by nuclear (AVT) did not show, excepting Lama 84 and Lama 87 cells, great variations and was not correlated with cell duplication rate. These results suggested that in cell lines the dispersion of NORs and their associated argyrophilic proteins reflect the rapidity of cell proliferation rather than the total volume fraction of the AgNOR aggregates. This point may appear quite surprising and is indeed difficult to interpret because it could be due to an imperfect stoichiometry in the precipitation reaction of the AgNORs proteins. However, after discriminant analysis, the nine cell lines can be classified into two groups: group 1: HL60, UM384, U937,

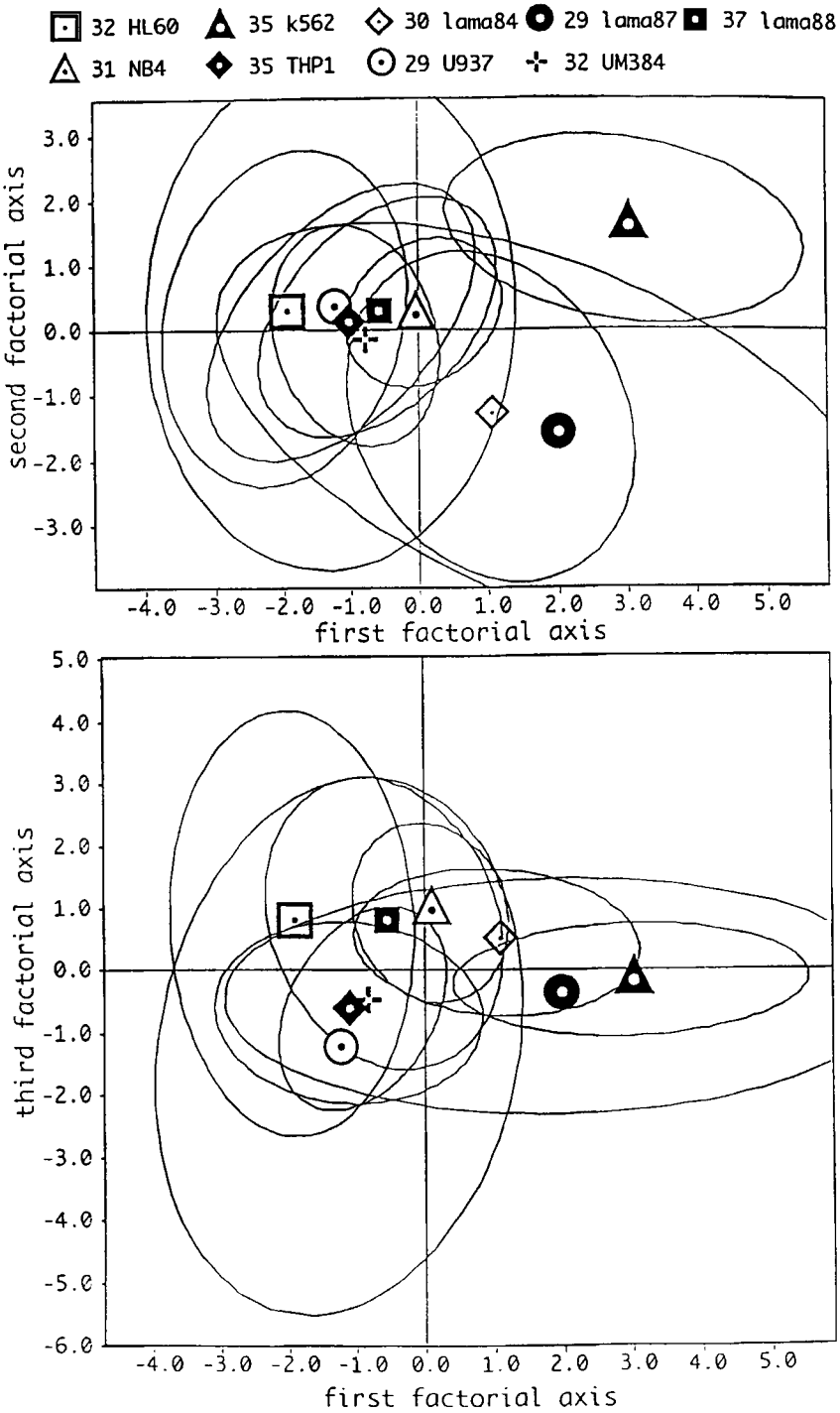

FIG. 11. Factorial discriminant analysis. Plots of the first and second factorial planes; the symbols are plotted at the central position of corresponding population and the ellipses are the 95% confidence limits of the population (in extenso 95% of the population can be found inside the ellipse).

LAMA 88, THP-1 and NB4 (slowly proliferating cells); group 2: LAMA 84, LAMA 87 and K562 (rapidly proliferating cells). The cells of the first group were differentiated along the granulomonocytic pathway and expressed only one or two differentiation potentialities: granulomonocytic (HL60, UM384 and NB4), eosinomonocytic (LAMA 88) or monocytic (THP-1 and U937). The cells of the second group were very undifferentiated and possessed three or more differentiation potentialities (erythrocytic, megakaryocytic, eosinophilic, granulo-

cytic, or monocytic). These results show a variation of AgNORs during the cell differentiation process. Experiments are in progress to confirm this relation between differentiation stages and AgNORs after culture of LAMA88 cells in presence of chemicals (TPA and sodium butyrate) and physiological (GM-CSF, TGFβ, erythropoietin, and vitamin D3) inducers.

AgNOR Analysis and Cytogenetical Study

It was demonstrated that the total number of chromosomes is positively correlated with the number of acrocentric chromosomes (25) and that the number of acrocentric chromosomes is correlated with the number of metaphase NORs (53). However, the majority of data published previously indicate the absence of a strict numerical relationship between the number of metaphase NORs and interphase AgNOR values (10, 12, 14, 53). It also has been shown that interphase AgNOR quantity is not related to the DNA ploidy in different cancer cells (14). However, in the present data the values of interphase AgNORs in leukemic cells were significantly correlated with metaphase NOR number and showed a positive trend with acrocentric chromosome number but not with total chromosome number. These observations indicate that a greater number of metaphase NORs could be associated with a greater number of interphase AgNORs and confirm that AgNORs is not related to DNA ploidy (14).

2D vs. 3D AgNOR Analysis

It was quite surprising that 3D analysis showed a underestimation of AgNORs quantity in comparison with 2D analysis, principally in rapidly proliferating cell lines. Furthermore, AgNOR areas computed in 2D showed a higher correlation with the speed of cell duplication than the AgNOR number computed under the same conditions. The lower number of AgNORs in 3D than in 2D in two cell lines is related to the differences of resolution and sometimes encountered "bizarre configurations" (26). The 3D AgNOR analysis offers a better resolution than 2D. The nucleus examined in spatial conditions obviate, moreover, the AgNOR masking effect. The AgNOR area measurements in 2D expressed the number of AgNOR aggregates rather than the actual amount of proteins. The mean of total volume fraction of AgNORs was not correlated with AgNOR area in 2D. These results are in agreement with previous data that showed that 2D AgNOR areas are related to cell duplication rate (14, 50) and ^{3}H-thymidine incorporation (10) independently of the type of neoplastic cells.

Analysis of Spatial Distribution Parameters

The analysis of 13 parameters of spatial distribution showed that AgNOR proteins are preferentially situated in central and equatorial plane. The AgNORs in the cells with greater proliferating ability had, generally, a larger number, a smaller average volume fraction, and a tendency to form clusters and move closer to the nuclear border. The study of the spatial distribution of AgNORs is also a new and interesting method to describe and distinguish the cells in their different proliferative and pathological states.

ACKNOWLEDGMENTS

The authors thank Dr. Victoria von Hagen for her advice in editing the manuscript.

LITERATURE CITED

1. Anderson TW, Stephens MA: Tests for randomness of directions against equatorial and bimodal alternatives. Biometrika 59:613–621, 1972.
2. Arden KC, Pathak S, Frankel LS, Zander A: AgNORs staining in human chromosomes: Differential staining in normal and leukemic bone-marrow samples. Int J Cancer 36:647–649, 1985.
3. Bertin E, Parazza F, Chassery JM: Segmentation and measurement based on 3D Voronoï: Application to confocal microscopy. Comput Med Imaging Graph 17:175–182, 1993.
4. Castleman KR: Digital image processing. In: Three-dimensional Image Processing, Oppenheim, AV (ed). Prentice Hall, Englewood Cliffs, NJ, 1979, pp 351–360.
5. Champelovier P, Seigneurin D, Leroux D, Micouin C, Kolodie L: Establishment and characterization of a granulocytic subclone (UM384) from the monoblastic cell line U 937. Exp Hematol 17: 779–784, 1989.
6. Champelovier P, Valiron O, Jacrot M, Leroux D, Seigneurin D: Selection and characterization of an erythroeosinophilic subclone (LAMA-87) and an eosinophilic subclone (LAMA-88) from the multipotential cell line LAMA-84. Leuk Res 18:903–918, 1995.
7. Charpin C, Andrac L, Devictor B, Habib M, Lavaut MN, Allasia C, Bonnier P, Piana L: Digital image analysis of nuclear morphometry, DNA ploidy and AgNORs in breast carcinoma cell imprints. Int J Oncol 3:949–956, 1994.
8. Crocker J, Macartney JC, Smith PJ: Correlation between DNA flow cytometric and nucleolar organiser regions data in non-Hodgkin's lymphomas. J Pathol 154:151–156, 1988.
9. Derenzini M, Betts CM, Ceccarelli C, Eusebi V: Ultrastructural organization of nucleoli in benign naevi and malignant melanomas. Virchws Arch Cell Pathol B 52:343–352, 1986.
10. Derenzini M, Pession A, Frabegoli F, Trerè D, Badiali M, Dehan P: Relationship between interphasic nucleolar organiser regions and growth rate in two neuroblastoma cell lines. Am J Pathol 134:925–932, 1989.
11. Derenzini M, Pession A, Trerè D: Quantity of nucleolar silver-stained proteins is related to proliferating activity in cancer cells. Lab Invest 63:137–140, 1990.
12. Derenzini M, Ploton D: Interphase nucleolar organizer regions in cancer cells. Int Rev Exp Pathol 32:149–192, 1992.
13. Derenzini M, Trerè D: Importance of nucleolar organizer regions in tumor pathology. Wirchws Arch Cell Pathol B 61:1–8, 1991.
14. Derenzini M, Trerè D, Chieco P, Melchiorri C: Interphase AgNOR quantity is not related to DNA content in 11 established human cancer cell lines. Exp Cell Res 211:282–285, 1994.
15. Egan MJ, Crocker J: Nucleolar organizer regions in tumor pathology. Br J Cancer 65:1–7, 1992.
16. Gallagher R, Collins S, Trujillo J, McCredie K, Ahearn M, Tsai S, Metzgar R, Aulakh G, Ting R, Ruscetti F, Gallo R: Characterization of the continuous, differentiating myeloid cell line (HL-60) from a patient with acute promyelocytic leukemia. Blood 54:713–733, 1979.
17. Giri DD, Nottingham JF, Lawry J, Dundas SAC, Underwood JC: Silver binding nucleolar organiser regions (AgNORs) in benign and malignant breast lesions: Correlation with ploidy and growth phase by DNA flow cytometry. J Pathol 157:307–313, 1989.
18. Goodpasture C, Bloom SE: Visualisation of nucleolar organiser regions in mammalian chromosomes using silver staining. Chromosoma 53:37–50, 1975.
19. Grotto HZW, Metze K, Lorand-Metze I: Pattern of nucleolar organizer regions in human leukemic cells. Analyt Cell Pathol 5:203–212, 1993.
20. Henderson AA, Warburton D, Atwood KC: Localisation of ribosomal

DNA in the human chromosome complement. Proc Natl Acad Sci USA 69:3394–3398, 1972.
21. Hernandez-Verdun D: The nucleolus today. J Cell Sci 99:465–471, 1991.
22. Hernandez-Verdun D, Robert-Nicoud M, Géraud G, Masson C: Behaviour of nucleolar proteins in nuclei lacking ribosomal genes: A study by confocal laser scanning microscopy. J Cell Sci 98:99–105, 1991.
23. Howell WM, Denton TE, Diamond JR: Differential staining of the satellite regions of human acrocentric chromosomes. Experientia 31:260–262, 1975.
24. Hsu TC, Spirito SE, Pradue ML: Distribution of 18+28S ribosomal genes in mammalian genomes. Chromosoma 53:25–36, 1975.
25. Hubbell HR, Hsu TC: Identification of nucleolus organizer regions (NORs) in normal and neoplastic human cells by silver staining technique. Cytogenet Cell Genet 19:185–196, 1977.
26. Imamura Y, Noriki S, Tsuzuki H, Nitta Y, Fukuda M: Fluorescent staining of nucleolar organiser regions for three-dimensional display by confocal laser scanning microscope. Eur J Histochem 37:321–328, 1993.
27. ISCN: Guidelines for cancer cytogenetics (Supp). International System for Human Cytogenetic Nomenclature, Mitelman F (ed), S. Karger, Basel, 1991.
28. Lanotte M, Martin-Thouvenin V, Najman S, Balerini P, Valensi F, Berger R: NB4, a maturation inducible cell line with t(15;17) marker isolated from a human acute promyelocytic leukemia (M3). Blood 77:1080–1086, 1991.
29. Lozzio CB, Lozzio BB: Human chronic myelogenous leukemia cell-line with positive Philadelphia chromosome. Blood 45:321–334, 1975.
30. Mamaev N, Mamaeva S, Liburkina I, Kozlova T, Medvedeva N, Makarkina C: The activity of nucleolar organiser regions of human bone marrow cells studied with silver staining: I. Chronic myelocytic leukaemia. Cancer Gen Cytogen 25:65–72, 1985.
31. Meehan SM, Fimls HM, Carney DN, Dervan PA: The diagnostic value of silver nucleolar organizer region assessment in breast cytology. Am J Clin Pathol 101:689–683, 1994.
32. Mourad WA, Pugh WC, Hun YO, Keating MJ: Cell kinetic analysis of interleukin-2 receptor tested chronic lymphocytic leukemia using the AgNOR silver stain. Am J Cin Pathol 101:300–304, 1994.
33. Nakamura S, Takeda Y, Okabe Y, Yoshida T, Ohtake S, Kobayashi K, Kanno M, Matsuda T: Argyrophilic proteins of nucleolar organizer region in acute leukemias and its relation to the S-phase fraction of leukemic cells. Acta Haematol 87:6–10, 1992.
34. Orita T, Kaijiwara K, Nishizaki T, Ikeda N, Kamiryo T, Aoki H: Nucleolar organizer regions in menigioma. Neurosurgery 26:43–46, 1990.
35. Parazza F, Bertin E, Wozniak Z, Usson Y: Analysis of the spatial distribution of AgNOR proteins in cell nuclei using simultaneous confocal scanning laser fluorescence and transmitted light microscopy. J Microsc 178:251–260, 1995.
36. Parazza F, Humbert C, Usson Y: Method for 3D volumetric analysis of intranuclear fluorescence distribution in confocal microscopy. Comput Med Imaging Graph 17:189–200, 1993.
37. Patterson MK: Measurement of growth and viability of cells in culture. In: Methods in Enzymology, Jakoby WB, Pastam IH (eds). Academic Press, New York, 1979, pp 141–152.
38. Ploton D, Gilbert N, Ménager M, Kaplan H, Adnet JJ: Three-dimensional co-localization of nucleolar argyrophilic components and DNA in cell nuclei by confocal microscopy. J Histochem Cytochem 42:137–148, 1994.
39. Ploton D, Menager M, Jeannesson P, Himber G, Pigeon F, Adnet JJ: Improvement in the staining and the visualisation of the AgNOR proteins (argyrophilic proteins of the nucleolar organiser region) at the optical level. Histochem J 18:5–14, 1986.
40. Ploton D, Menager M, Lechki C, Jeannesson P, Visseaux S, Adnet JJ: Coloration des organisateurs nucleolaires (NORs) par l'argent. Application à l'etude de la structure du nucléole et interêts en pathologie. Ann Pathol 3:248–252, 1988.
41. Pradue ML, Hsu TC: Location of 18S and 28S ribosomal genes of the Indian Muntjac. J Cell Biol 64:251–254, 1975.
42. Rentrop M, Knapp B, Winter H, Schweizer J: Aminoaklysilane-treated glass slides as support for in situ hybridization of keratin cDNAs to frozen tissue sections under varying and pretreatment conditions. Histochem J 18:271–276, 1986.
43. Robert-Fortel I, Junéra HR, Géraud G, Hernandez-Verdun D: Three-dimensional organization of the ribosomal genes and Ag-NOR proteins during interphase and mitosis in PtK1 cells studied by confocal microscopy. Chromosoma 102:146–157, 1993.
44. Rosa J, Mehta A, Filipe M: Nucleolar organiser regions, proliferative activity and DNA index in gastric carcinoma. Histopathology 16: 614–616, 1990.
45. Sato Y, Abe S, Kubota K, Sasaki M, Miura Y: Silver-stained nucleolar organizer regions in bone marrow cells and peripheral blood lymphocytes of Philadelphia chromosome-positive chronic myelocytic leukaemia patients. Cancer Genet Cytogen 23:37–45, 1986.
46. Seigneurin D, Champelovier P, Mouchiroud G, Berthier R, Leroux D, Prenent M, McGregor J, Starck J, Morle F, Micouin C, Pietrantuono A, Kolodie L: Human chronic myeloid leukemic cell line with positive Philadelphia chromosome exhibits megacaryocytic and erythroid characteristics. Exp Hematol 15:822–832, 1987.
47. Stocker AJ: Correspondence of silver banding with rRNA hybridization sites in polytene chromosomes of Rhynchosciaria hollanderi. Exp Cell Res 114:429–434, 1978.
48. Sundstrom C, Nilsson K: Establishment and characterization of a human histiocytic lymphoma cell line (U937). Int J Cancer 17:565–577, 1976.
49. Trerè D: Critical analysis of the methods commonly employed in the assessment of cell proliferation: advantages of the NOR silver-staining technique in routine cyto-histopathology. Anal Cell Pathol 5:191–201, 1993.
50. Trerè D, Pession A, Derenzini M: The silver-stained proteins of interphasic nucleolar organizer regions as a parameter of cell duplication rate. Exp Cell Res 184:131–137, 1989.
51. Takahashi H, Fujita S, Okabe H: Estimation of silver-binding nucleolar organizer regions (AgNORs) in lymphoproliferative disorders of gastrointestinal tract. Path Res Pract 190:350–361, 1994.
52. Tsuchiya S, Yamabe M, Yamaguchi Y, Kobayashi Y, Konno T, Tada K: Establishment and characterization of a human acute monocytic leukemia cell line (THP-1). Int J Cancer 26:171–176, 1980.
53. Trent JM, Carlin DA, Davis JR: Expression of silver-stained nucleolar organizing regions (AgNORs) in human cancer. Cytogenet Cell Genet 30:31–38, 1981.
54. Wachtler F, Stahl A: The nucleolus: A structural and functional interpretation. Micron 24:473–505, 1993.
55. Wozniak ZM, Bonnefoix T, Zheng X. Seigneurin D, Sotto JJ: Interest of argyrophilic proteins nucleolar organizer regions (AgNOR) to estimate the reactivity of T cell clones against autologous malignant B-NHL cells. Anal Cell Pathol 9:123–133, 1995.